INTERNATIONAL JOURNAL OF CONSERVATION SCIENCE

ISSN: 2067-533X Volume 8, Issue 2, April-June 2017: 167-176 www.ijcs.uaic.ro

LIMESTONE REPLACEMENT IN RESTORATION: THE CASE OF THE CHURCH OF SANTA MARIA (BIRKIRKARA, MALTA)

Lino BIANCO*

Department of Architecture and Urban Design, Faculty for the Built Environment, University of Malta, Msida MSD 2080, Malta

Abstract

The Church of Santa Maria is one of the finest examples of seventeenth century heritage monuments in the Maltese archipelago. The provenance of limestone used in the restoration works is different from the original heritage fabric. It is obtained from a quarry located 5.2 km south of the church whilst the original source of the limestone, according to tradition, is from an area 2.2 km north of the monument. This petrological study concludes that although both extracted from the same geological formation, there are physical, textural, geochemical and mineralogical differences even over a distance of 7.4 km. The limestone used in replacement is more resistance in terms of compressive strength and is less porous. Although having same principal non-carbonate oxides, the quantitative variations in the geochemistry and the mineralogy are indicative of qualitative differences between the two lithotypes; they are diagnostic indicators of the provenance of the limestone.

Keywords: *Limestone; Globigerina Limestone; Restoration; Compatibility, Evaluation, Baroque; Malta; Birkirkara.*

Introduction

Birkirkara is the largest settlement in mainland Malta. The Church of Santa Maria, locally referred to as the Old Church, (UTM coordinates: 14.46367, 35.89624; WGS84 coordinates: 14.46302, 35.89503), is the former parish church of the town and an outstanding example of ecclesiastical early Baroque architecture of Malta (Fig. 1, left). It was designed in circa 1600 by Vittorio Cassar, the son of the architect who was responsible for the design of the Conventual Church of the Knights of the Order of St John in the capital Valletta. Its construction spanned over six decades. Although the interior of the church is richly carved and decorated, the exterior is plain except for the elevation of the main entrance which recalls the Church of Santi Spiritus at Salamanca and the Pellejeria door of Burgos Cathedral, both in Spain [1]. This elevation, introduced by Tommaso Dingli in 1617, is the finest part of the building. It is influenced by the retrograde Renaissance style of the sixteenth century executed in Vitruvian language. Once the new parish of Birkirkara was completed in 1745, the Church of Santa Maria was allowed to fall in to disrepair and, until restoration commenced in 1969, was a partial ruin. Although more than three and a half centuries had lapsed, the original carvings on

* Corresponding author: lino.bianco@um.edu.mt

the elevation have weathered well and the acanthus capitals are crisp and sharp (Fig. 1, right). It is entirely constructed of Lower Globigerina Limestone, the oldest stratigraphy of the Globigerina formation, a Miocene carbonate sedimentary limestone of shallow marine origin.

Fig. 1. The Church of Santa Maria; the location of the springer which is covered by this study is indicated in red (left) and a well weathered acanthus capital (right)

The selection of dimension stone is critical in the preservation and restoration of built heritage [2-4]. During the period of the Knights of St John (1530-1798) the selection of limestone was not just restricted by availability and suitable technology but also by the designated properties required [5].

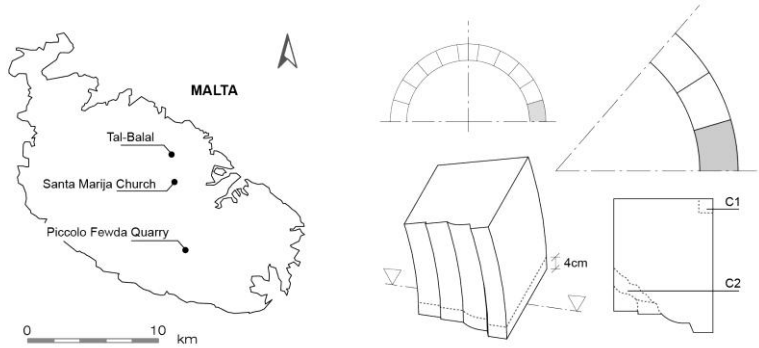

Fig. 2. Site location map (left) and position of C samples from the original, replaced springer (right)

An important consideration in heritage buildings is the provenance of limestone used in their erection [6-9]. Although the exact location of the historic quarry used to supply the limestone for the construction of the church is not known, according to tradition it was located in the limits of Tal-Balal (UTM coordinates: 14.46363, 35.91616; WGS84 coordinates: 14.46298, 35.91496), 2.2 km north (Fig. 2, left). At the time of the restoration works undertaken in the 1990s, quarrying areas extracting the Lower Globigerina Limestone in Malta were at Tal-Balal and Mqabba [10]. Instead of utilizing limestone from the former, the latter was selected to

replace the deteriorated heritage fabric as it was the best quality limestone on the market at the time. This paper is based on a study of the characteristics of this limestone. A spectrum of analytical tests was undertaken to establish the properties of the original building fabric.

Materials and methods

The limestone used in the construction of the church represented the building stone available at the time. The original weathered stone is considerably harder; it had withstood the elements and the number of dimension stones requiring replacement was minimal. The areas most affected are the lower courses up to circa 1.8 metres above present ground level, the area prone to rising damp. The professionals involved in the restoration works selected Piccolo Fewda quarry located on the outskirts of Mqabba (UTM coordinates: 14.47091, 35.84992; WGS84 coordinates: 14.47026, 35.84871), 5.2 km south of the church (Fig. 2, left).

The samples analyzed are listed in Table 1. The church samples are derived from a replaced springer (Fig. 1, left and Fig. 2, right). In the opinion of the author, the only reason which justified its replacement was aesthetical compatibility with the surrounding fabric because, otherwise, the limestone seemed structurally sound. The samples from the quarry were identified by its owner Salvu Bondin, the third generation working in the industry and former president of the quarry association (of Malta). He had been involved in the mineral extractive industry for circa six and a half decades. No details regarding the horizons of these samples were unavailable.

Table 1. Sample descriptions

Source	Code	Description of sample
Church	C1	Springer stone, undeteriorated surface
Church	C2	Springer stone, deteriorated surface
Quarry	Q1	Limestone referred by quarry owner as 'first' quality; it is the limestone used in the restoration work
Quarry	Q2	Limestone referred by quarry owner as identical to Q1 but seasoned for 12 years
Quarry	Q3	Limestone referred by quarry owner as 'second' quality. According to him this limestone, which contains a lot of glass fragments, is suitable for dimension stone provided that it is used at least 2 courses (circa 60cm) above the damp proof course.

The petrographical characterization of the samples was established through petrophysical, textural, geochemical and mineralogical analysis. The physical properties assessed were apparent density, uniaxial compressive strength (Avery-Denison model) and ultrasonic pulse velocity (PUNDIT model). Tests were undertaken on oven dried (temperature $105^{+}/-5^{o}$C) and saturated (fully submerged for 24 hours) samples. In case of sample C1, a cube measuring 40x40x40mm could only be secured; C2 was fragile and broke up during sample preparation. Correlation exists between uniaxial compressive strength and ultrasonic pulse velocity [11].

Petrographical microscopy, scanning electron microscopy (Hitachi S-520 model), and mercury intrusion porosimetry (Quantachrome SP-33B) were used to obtain information on the texture. The scanning electron microscope was equipped with energy dispersive analyser. Thin section analysis was carried out to study the cement fabric, porosity and permeability. All

sections were impregnated with dyed blue araldite so that the pore structure could be easily observed. Scanning electron microscopy was used to study the texture, the cementing fabric, the microphotograph pores, and the non-carbonate fraction remaining on the filter paper [12-13]. Mercury intrusion porosimeter was used to obtain a quantitative classification of the pores. Porosimetry reflects the proportion of voids contained; information is not planar but volumetric. In calculating the pore number fraction, pores were assumed to be cylindrical and equal in length.

Chemical analysis was determined through loss-on-ignition and x-ray fluorescence analysis. Loss on ignition is the traditional analytical chemical method to estimate the organic and carbonate content of sediments [14]. An ARL 8420+ X-ray fluorescence spectrometer was used on pressed powder pellets to determine the bulk chemistry [15]. The mineralogical techniques employed were acid insoluble residue and x-ray diffraction. The former was used to quantitatively estimate the non-carbonate fraction. X-ray diffraction (Philips PW1729 X-ray generator) analysis was performed on this fraction to establish the mineralogical composition of the residue. Through the analysis of the filter paper containing the acid insoluble residue, the non-carbonate constituents were identified. X-ray diffraction was also used to determine the mineralogy of whole rock powder and of its clay fraction. A semi-quantitative data of each mineral present is given by its respective relative intensity. Oriented mount technique was used for the clay fraction since the d001 peaks are enhanced [16].

Results and Discussions

Petrophysical characteristics

The variation between the apparent density (oven dried and saturated) of the C sample and the Q samples is minimal (Table 2). The compressive strength (oven dried and saturated) and the USPV (perpendicular and parallel to the bedding plan) for the church sample are lower than those of the quarry. The difference between first quality, seasoned lithotype, and the second quality limestone was minimal. Same holds for USPV.

The uniaxial compressive strength for the C and Q samples at 17.1N/mm^2 and at an average of 26.5N/mm^2 respectively falls in the 15 to 37.5N/mm^2 range stated in national structural handbook [17]. A comprehensive study undertaken in the late nineteenth century on the resistance of local stone to thrusting stress [18] included 10 samples from Ta` Marozz quarry, at Tal-Balal, which registered an average crushing strength of 17.98N/mm^2. Although not a criterion for limestone quality assessment, this is closer to the compressive strength of the church sample.

Table 2. Physical properties

Code	Apparent Density (kg/m^3)		Compressive strength (N/mm^2)		USPV (km/s)	
	oven dried	*saturated*	*oven dried*	*saturated*	*perpendicular*	*Parallel*
C1	1717.70	1939.07	17.12	10.78	2.62	2.68
C2	n.a.	n.a.	n.a.	n.a.	n.a.	n.a.
Q1	1725.06	1992.13	29.52	18.59	3.09	3.00
Q2	1692.93	1955.13	24.84	15.22	3.01	2.88
Q3	1799.01	2021.20	25.04	14.72	3.00	2.96

n.d.: not available.

Textural characteristics

Porosity in all samples is intra and inter-particle type. In the undeteriorated church sample C1, the rock matrix is unevenly distributed biomicrite. Burrows, 1 to 1.5 mm diameter, cut irregularly across the fabric. Burrow infill is wackestone. Bio-retexturing introduces unlithified sediment of variable permeability in the host rock [19]. Most allochems are cemented by fine grained sparry calcite which imperfectly fills the inter particle voids (Fig. 3, left). There are numerous randomly distributed 20 μm diameter intra-particle pores. Ill defined area of high permeability is present away from the burrows and within the host rock. Grain packing in these areas is about the same as in the lower permeability areas but generally is lacking micrite and spar cement. Principal components are planktonic (maximum 160 μm diameter) and sparse bentonic foraminifera. Rare echinoid fragments are also present. Intermediate bioclasts comprise about 50% of the allochems. Undamaged allochems have unfilled chambers. Quartz, glauconite and some iron oxide are also present. Glauconite and oxide grain boundaries are ill defined. These minerals have started to break down. Staining of the fabric is present. Some of the non-carbonate oxides were captured through microphotographing the insoluble residue retained on the filter paper (Fig. 3, right).

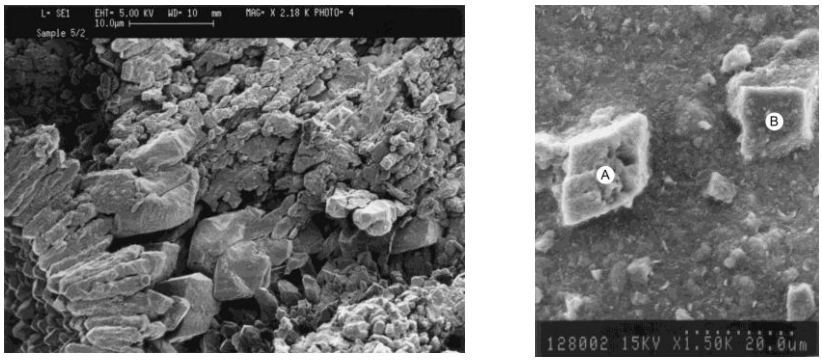

Fig. 3. Scanning electron images of sample C1 showing the mechanical interlocking and pores filled with cement (left) and non-carbonate fraction (A: feldspar, B: quartz) of the insoluble residue retained on the filter paper (right)

C2 is packed biomicrite with over 50% allochems. A burrow, mean diameter of about 1.25 mm, cut across the matrix. Sparse micrite forms burrow infill. Allochems are cemented by fine-grained spary calcite. Effective porosity along grain boundaries is more predominant in the host rock then in the burrow infill. Principal components include undamaged globigerinoids (25%), shell fragments, and various randomly distributed mafic minerals. Rounded glauconite grains and elongated monocrystalline quartz grains are less than 50 μm and 80 μm respectively. Rounded quartz grains are also present. Staining of some grains by weathering iron oxide/s or iron oxide/s in solution is/are present. Weathering and staining of a secondary green/grey mineral is also present. It is likely to be glauconite breaking down. Stains are unidirectional and perpendicular to bedding.

The fabric of the Q samples is well-sorted intrabiosparite wackestone (Fig. 4). Allochems are cemented with sparry calcite. Such calcite is present on the inside rims of unbroken, unfilled allochem chambers (Fig. 4). Random, 10 μm diameter, intraparticle voids occur in the sparry calcite. A few 150 μm diameter impregnated pores are also present.

Foraminifera make up most of the host rock. Undamaged, unfilled globigerina chambers, mean diameter of 50 μm, comprise a quarter of the sediment. Quartz and feldspar are present, the former accounting for the glass fragments which the quarry owner had made reference to. The main constituents of lithotype Q3 are unbroken, unfilled, allochems (25%), fossil fragments (maximum size 7.1 mm), monocrystalline quartz, feldspar, glauconite and iron oxide. Quartz grains, occasionally present in clusters, are 70 μm and angularly shaped. Maximum size of feldspar is 55 μm. Glauconite grains, 150 μm in diameter, are not breaking down. Staining is present where clusters of iron oxide minerals are breaking down. Occasional staining by iron oxide in solution is present.

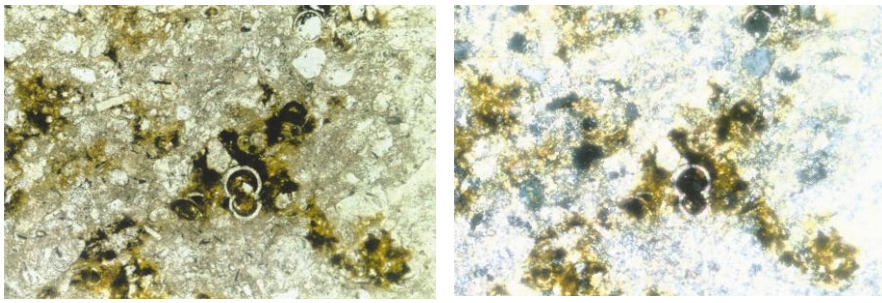

Fig. 4. Thin section of Lower Globigerina Limestone in plane polarized light (left) and crossed polars (right) showing the foraminiferal wackestone predominately consisting of globigerina grains and echinoid fragments

Mercury intrusion porosimetry establish the volumes and radii of pores within the fabric [20-21]. The raw intruded volume obtained was normalised by dividing the volume of mercury by the weight of the sample. The interpolated volume for each sample analysed is given in Table 3. The samples from the church and the first quality quarry stone have higher volume of pores whilst the second quality limestone is about 20% less. The distribution of the pores in the C sample and the Q samples indicates petrographical variation indicative of the provenance of the limestone.

Table 3. Interpolated mercury intrusion pore diameter

Code	Volume of pores (cm^3/g)			Total (cm^3/g)
	Pore radius			
	> 40000Å	***40-40000Å***	***< 40Å***	
C1	0.0091	0.1120	0.0005	0.1216
C2				
Q1	0.0073	0.1000	0.0003	0.1076
Q2	0.0014	0.1133	0.0001	0.1148
Q3	0.0011	0.0889	0.0006	0.0906

Geochemistry and mineralogical characteristics

The geochemical composition of the C samples varies from the Q samples (Table 4). For the scope of accuracy and precision of the data retrieved, values are given to three decimal places. Second quality limestone has higher non-carbonate content than first quality Q samples and a carbonate content equivalent to the C samples. The main non-carbonate fraction in all samples is SiO_2; the mean in the C samples is 4.96% whilst the second quality Q2 sample, at 6.4%, is twice the first quality stone (Fig. 5). The C samples registered lowest Al_20_3 and highest

MgO contents. Variation may be due to change in allochem mineralogy [22]. Fe_2O_3 is similar in all samples except for the second quality one which is about 250% higher. K_2O is higher in the Q than the C samples with the second quality having twice the first. The variation of the P_2O_5 and TiO_2 is similar to SiO_2 and K_2O respectively with the latter being 200% higher in the second quality limestone. Na_20 is circa 0.05+/-0.01% except for the freshly quarried stone which is negligible. MnO is present in traces of 0.031+/-0.01% in the C samples but absent in the Q samples.

Table 4. X-ray fluorescence analysis.

Code	CaO	SiO_2	Al_2O_3	MgO	Fe_2O_3	K_2O	P_2O_5	TiO_2	Na_2O	MnO	LOI
C1	50.079	4.945	0.678	1.154	0.343	0.246	0.238	0.087	0.062	0.030	42.517
C2	49.943	4.749	0.620	1.158	0.333	0.265	0.236	0.085	0.041	0.032	42.453
Q1	52.860	3.280	0.970	0.840	0.360	0.289	0.123	0.090	<LOD	0.000	42.474
Q2	52.490	3.060	0.910	0.850	0.310	0.259	0.148	0.080	0.050	0.000	42.643
Q3	50.140	6.380	1.570	0.910	0.910	0.525	0.294	0.180	0.010	0.000	40.398

Totals for each of the samples analysed for the quarry was in the region of $100^{+}1\%$.

X-ray diffraction analysis of the whole rock recorded the presence of quartz in all C and Q samples (Table 5). The mineralogy of the insoluble residue is mainly quartz and K-feldspar. Muscovite, kaolinite, illite and smectite were detected. The second quality limestone contains goethite. This mineral occurs as weathering product of iron bearing minerals such as pyrite and is usually formed under oxidising conditions. It is one of the hydroxides and oxides of iron grouped as limonite. The mineralogy of the clay fraction of all samples is kaolinite, illite, smectite, quartz and K-feldspar. Smectite and illite are structurally related to micas. Most of the inter layer water of smectites is lost on heating to 335^{o}C. Illite differs from muscovite in having less potassium and more silica [23]. Illite can form during diagenesis by alteration of other clay species or be the result of post depositional weathering of muscovite and silicates, notably feldspars. Kaolinite is a byproduct of the weathering of feldspars and other silicates. Glauconite, a mineral noted in thin sections, was not detected in X-ray diffraction.

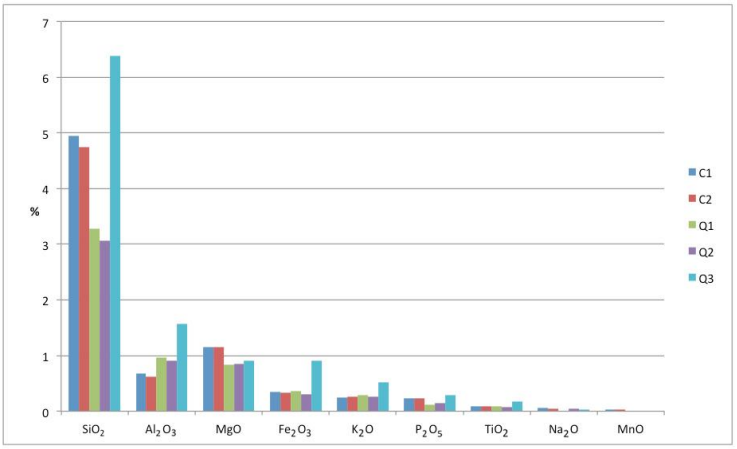

Fig. 5. Non-carbonate fraction of the C and Q samples.

Table 5. X-ray diffraction analysis: Summary of identified minerals.

Code	Whole rock		Insoluble residue								Clay fraction		
	Cal	*Qtz*	*Qtz*	*Kfs*	*Ms*	*Kln*	*ill*	*Sme*	*Gp*	*Gt*	*Kln*	*ill*	*Sme*
C1	x	x	x	x	x						x	x	x
C2	x	x	x	x	x	x	x		x		n.d.	n.d.	n.d.
Q1	x	x	x	x	x	x					x	x	x
Q2	x	x	x	x		x		x		x	x	x	x
Q3	x	x	x	x		x		x			x	x	x

n.d.: not detected.

Conclusions

The limestone used in the restoration works at the old church of Santa Maria has significant different characteristics from the original heritage fabric. The compositional differences of the limestone are diagnostic of the provenance. Although extracted from the same lithological formation, it is petrological diverse; the physical, textural, geochemical and mineralogical compositions are quantitatively different thus giving rise to qualitative different properties. The following findings merit noting:

1. The first quality quarry lithotype is more stress resistant than the C samples. The compressive strength of the Lower Globigerina Limestone formation varies. The limestone originally used in the old church is on the lower side of the range and it does correspond to historical, official analytical results undertaken in the late nineteenth century on a quarry from Tal-Balal area;
2. The church sample is more porous than the quarry samples, the bulk being in the range of 40-40000 Å. Passage of water through the matrix encouraged the growth of the post depositional interlocking calcite crystal fabric present in the C sample. These crystals provide the mechanical bonding which accounts for the durability of the building stone;
3. The principal non-carbonate oxides are SiO_2, Al_2O_3, Fe_2O_3, and K_2O. Arguing that the C samples have a geochemistry composition akin to the second quality Q lithotype is not a correct interpretation. Variations in the non-carbonate indicate differences in the lithology of the C and Q samples; and
4. Applying XRD data and microphotographs of the insoluble residue, the principal non-carbonate oxides are attributed to quartz, clays, K-feldspar, muscovite, and some iron oxide mineral(s). These are highest in the second quality lithotype. The variations are quantitative. The C samples have higher quartz but less clays than the first quality lithotype from the quarry; the muscovite content is higher than the Q samples.

Selecting limestone for replacement on the basis of crushing strength is rudimentary. A consideration for the effectiveness of restoration intervention is compatibility of the limestone replacing the original fabric. Compatibility has bearing on the durability of the works undertaken. Textural, geochemistry and the corresponding mineralogy variations are indicators of the original sediment of deposition.

Acknowledgments

This study forms part of postgraduate research undertaken at the University of Leicester under the supervision of Dr H. M. Pedley and through the guidance of late Prof. Anselm Dunham. It was financially supported by the Oil Exploration Division, Office of the Prime Minister, Malta.

References

[1] J. Quentin Hughes, **The Building of Malta during the period of the Knights of St John of Jerusalem**, Alec Tiranti, London, 1967.

[2] P. Wagner, R. Holzer, M. Bednarik, M. Laho, *Building stone selection for the restoration of historic objects*, **Acta Geologica Slovaca, 1**(1), 2009, pp. 9-14.

[3] R. Reucher, H. Leisen, E. Von Plehwe-Leisen, R. Kleinschrodt, *The building stones of the Khmer-temple at Angkor/Cambodia: A petrological and geochemical approach towards a conservationoriented characterisation of the inventory*, **Geochimica et Cosmochimica Acta, 71**(15), Suppl S, 2007, pp. A834-A834.

[4] W.J. (Wido) Quist, *Replacement of natural stone in conservation of historic buildings: Evaluation of replacement of natural stone at the church of Our Lady in Breda*, **Heron, 54**(4), 2009, pp. 251-278. http://repository.tudelft.nl/islandora/object/uuid:339866d6-1496-4bac-b407-c718bd99ef99? collection=research, [accessed online 06.04.2016].

[5] L. Bianco, *Geocultural activity in seventeenth and eighteenth century Malta*, **GeoJournal**, **48**(4), 1999, pp. 337-340.

[6] C. Uhlir, K. Schaller, M. Unterwurzacher, *Historic Quarries: Case Studies*, **Scientific Computing and Cultural Heritage: Contributions in Computational Humanities** (Editors: H.G. Bock, W. Jäger and M.J. Winckler), Springer, Heidelberg, 2013, pp. 245-253.

[7] R. Navarro, J. Sánchez-Valverde, J.M. Baltuille, *The Natural Stone in the Historic Buildings of the City of Granada (Southern Spain). Features as a Possible Candidate for the Designation of "Global Heritage Stone Province"*, **Engineering Geology for Society and Territory, 5,** 2015, pp. 229-232.

[8] E. Torrero, D. Sanz, M.N. Arroyo, V. Navarro, *The Cathedral of Santa Maria (Cuenca, Spain): Principal stone characterization and conservation status*, **International Journal of Conservation Science, 6**(4), 2015, pp. 625-632.

[9] L. Bianco, *Techniques to determine the provenance of limestone used in Neolithic Architecture of Malta*, **Romanian Journal of Physics, 62** (901), 2017, pp. 1-10.

[10] D.H. Camilleri, *Globigerina limestone as a structural material*, **The Architect,** March 1988, pp. 17-25.

[11] E. Vasanelli, D. Colangiuli, A. Calia, M. Sileo, M.A. Aiello, *Ultrasonic pulse velocity for the evaluation of physical and mechanical properties of a highly porous building limestone*, **Ultrasonics, 60,** 2015, pp. 33–40.

[12] S.J.B. Reed, **Electron Microprobe Analysis and Scanning Electron Microscopy in Geology** (second edition), Cambridge University Press, Cambridge, 2005.

[13] K. Pye, *Forensic examination of rocks, sediments, soils and dusts using scanning electron microscopy and X-ray chemical microanalysis*, **Forensic Geoscience: Principles, Techniques and Applications** (Editors: K. Pye and D.J. Croft), 232, Special Publications, Geological Society, London, 2004, pp. 103–122.

[14] W.E. Dean, *Determination of carbonate and organic matter in calcareous sediments and sedimentary rocks by loss on ignition: comparison with other methods*, **Journal of Sedimentary Petrology, 44,** 1974, pp. 242–248.

[15] G. Fitton, *X-ray fluorescence spectrometry*, **Modern Analytical Geochemistry** (Editor: R. Gill),, Longman, Harlow, 1997, pp. 97–115.
[16] J.I. Drever, *The Preparation of Oriented Clay Mineral Specimens for X-ray Diffraction Analysis by a Filter-Membrane Peel Technique*, **American Mineralogist, 58,** 1973, pp. 553-554.
[17] D.H. Camilleri, **Structural Integrity Handbook: Building-Regulations 2000**, Building Industry Consultative Council, Malta, 2000. http://www.dhiperiti.com/wp-content/uploads/2013/10/2.Structural-Integrity-Handbook-Building-Regulations-20006.pdf, [accessed online 22.01.2016].
[18] * * *, The Crown Agents for the Colonies, **Resistance of Malta and Gozo Stone to Thrusting Stress**, David Kirkaldy & Son, London, 1885.
[19] H.M. Pedley, *Bio-retexturing: early diagenetic fabric modifications in outer-ramp settings - A case study from the Oligo-Miocene of the Central Mediterranean*, **Sedimentary Geology, 79,** 1992, pp. 173-188.
[20] V. Cnudde, A. Cwirzen, B. Masschaele, P.J.S. Jacobs, *Porosity and microstructure characterization of building stones and concretes*, **Engineering Geology, 103,** 2009, pp. 76–83.
[21] Z. Yan, C. Chen, P. Fan, M. Wang, X. Fang, *Pore Structure Characterization of Ten Typical Rocks in China*, **The Electronic Journal of Geotechnical Engineering, 20**(2), 2015, pp. 479-494.
[22] M.E. Tucker, **Sedimentary Petrology: An Introduction to the Origin of Sedimentary Rocks** (third edition), Blackwell Science Ltd, Oxford, 2001.
[23] M.R. Leeder, **Sedimentology: Process and Product** (first edition), Chapman & Hall, London, 1982, reprinted 1994.

Received: August 02, 2016
Accepted: May 27, 2017